



HAL
open science

A Two-Fold Increase of Phosphorus in Alpine Ice Over the Twentieth Century: Contributions From Dust, Primary Biogenic Emissions, Coal Burning, and Pig Iron Production

Michel Legrand, Joseph Mcconnell, Gilles Bergametti, Andreas Plach, Karine Desboeufs, Nathan Chellman, Susanne Preunkert, Andreas Stohl

► To cite this version:

Michel Legrand, Joseph Mcconnell, Gilles Bergametti, Andreas Plach, Karine Desboeufs, et al.. A Two-Fold Increase of Phosphorus in Alpine Ice Over the Twentieth Century: Contributions From Dust, Primary Biogenic Emissions, Coal Burning, and Pig Iron Production. *Journal of Geophysical Research: Atmospheres*, 2023, 128 (19), 10.1029/2023JD039236 . hal-04241336

HAL Id: hal-04241336

<https://hal.science/hal-04241336>

Submitted on 13 Oct 2023

HAL is a multi-disciplinary open access archive for the deposit and dissemination of scientific research documents, whether they are published or not. The documents may come from teaching and research institutions in France or abroad, or from public or private research centers.

L'archive ouverte pluridisciplinaire **HAL**, est destinée au dépôt et à la diffusion de documents scientifiques de niveau recherche, publiés ou non, émanant des établissements d'enseignement et de recherche français ou étrangers, des laboratoires publics ou privés.

JGR Atmospheres

RESEARCH ARTICLE

10.1029/2023JD039236

Key Points:

- A doubling of phosphorus in Alpine ice deposited between 1850 and 2000 from increasing natural and anthropogenic emissions
- Phosphorus deposition trends from 1900 to 1975 mainly attributed to coal burning and pig iron industry emissions
- Natural European phosphorus sources dominated by primary emissions of biogenic (70%) and dust (30%) particles that were enhanced after 1975

Supporting Information:

Supporting Information may be found in the online version of this article.

Correspondence to:

M. Legrand,
michel.legrand@lisa.ipsl.fr

Citation:

Legrand, M., McConnell, J. R., Bergametti, G., Plach, A., Desboeufs, K., Chellman, N., et al. (2023). A two-fold increase of phosphorus in Alpine ice over the twentieth century: Contributions from dust, primary biogenic emissions, coal burning, and pig iron production. *Journal of Geophysical Research: Atmospheres*, 128, e2023JD039236. <https://doi.org/10.1029/2023JD039236>

Received 10 MAY 2023

Accepted 16 SEP 2023

Author Contributions:

Conceptualization: Michel Legrand,

Joseph R. McConnell

Formal analysis: Michel Legrand,

Joseph R. McConnell, Gilles Bergametti, Andreas Plach, Karine Desboeufs, Nathan Chellman, Susanne Preunkert, Andreas Stohl

Investigation: Michel Legrand, Joseph R. McConnell, Gilles Bergametti, Andreas Plach, Karine Desboeufs, Nathan Chellman, Susanne Preunkert, Andreas Stohl

Methodology: Michel Legrand, Joseph R. McConnell, Gilles Bergametti, Andreas Plach, Karine Desboeufs, Nathan Chellman, Susanne Preunkert, Andreas Stohl

A Two-Fold Increase of Phosphorus in Alpine Ice Over the Twentieth Century: Contributions From Dust, Primary Biogenic Emissions, Coal Burning, and Pig Iron Production

Michel Legrand^{1,2} , Joseph R. McConnell³ , Gilles Bergametti¹ , Andreas Plach⁴ ,
Karine Desboeufs¹, Nathan Chellman³ , Susanne Preunkert² , and Andreas Stohl⁴

¹Université Paris Cité and University Paris Est Creteil, CNRS, LISA, Paris, France, ²Université Grenoble Alpes, CNRS, Institut des Géosciences de l'Environnement (IGE), Grenoble, France, ³Division of Hydrologic Sciences, Desert Research Institute, Reno, NV, USA, ⁴Department of Meteorology and Geophysics, University of Vienna, Vienna, Austria

Abstract Phosphorus (P) is a key nutrient for many organisms but its global atmospheric budget is largely unconstrained. Estimates of major emissions sources such as fossil-fuel combustion range from ~0.02 to 1.1 Tg yr⁻¹, and primary biogenic emissions range from 0.16 to 1.0 Tg yr⁻¹. Here we used detailed measurements of phosphorus in Alpine ice cores extracted from the Col du Dôme (CDD) glacier located near the Mont Blanc summit and atmospheric model simulations to evaluate changes in western European emissions from pre-industrial (PI) to modern times. The ice-core records show that P concentrations during the PI were about 0.9 ng g⁻¹, of which one third was of crustal origin and two thirds the result of primary biogenic emissions. Concentrations were higher throughout the 20th century, reaching 2.5 ng g⁻¹ in the 1980s. Analysis of source tracers measured in the same ice, commodity productions statistics, and other information suggest that the increase in P throughout the 20th century was caused by enhanced emissions from natural and anthropogenic sources. Coal burning and steel industry represented the main anthropogenic sources during the first and second half of the century, respectively. After 1950, the increase in P was also caused by enhanced dust emissions, with increased biogenic emissions caused by recent changes of use-land also contributing. These findings provide important constraints on the atmospheric P budget at the scale of western Europe during the recent centuries.

Plain Language Summary Phosphorus is an important nutrient for terrestrial and aquatic flora and fauna. Whereas dust aerosol emissions are the dominant atmospheric source of phosphorus on a global scale, other sources such as biogenic particles emitted by vegetation, as well as fossil-fuel combustion, may represent important sources in less-dusty industrialized regions. Estimates of these non-crustal sources are uncertain, however, with values often varying by an order of magnitude or more. Comparison with long-term pollution records extracted from well-dated ice cores provides a means of evaluating these estimates. Here, we analyzed phosphorus in ice cores extracted near the Mont Blanc summit in the French Alps to develop an 1850 to 2000 record. Phosphorus deposition doubled during this period, with increases attributed to enhancement of both natural (dust and biogenic particles emitted by vegetation) and anthropogenic (mainly coal burning and the steel industry) emissions.

1. Introduction

Phosphorus (P) is an important and often limiting nutrient in many marine and continental ecosystems. First pointed out by Broecker (1982), enhanced deposition of dust over the ocean during ice ages may have fertilized marine biota, and thus modulated long-term changes in atmospheric carbon dioxide (CO₂) concentrations. Modern global warming-related changes in climate and land cover probably have modified terrigenous P exported from continent regions. Human activities also have impacted the atmospheric P cycle. In addition to the fertilizer industry and fertilizer application, several high-temperature processes including coal burning and pig iron production emit significant amounts of P into the atmosphere, too.

Up to now, five studies have provided estimates of the present-day P budget at the global scale (Brahney et al., 2015; Graham & Duce, 1979; Mahowald et al., 2008; Myriokefalitakis et al., 2016; Wang et al., 2015). In addition, Wang et al. (2015) investigated changes of the budget from 1960 to 2000, while Brahney et al. (2015) and Myriokefalitakis et al. (2016) evaluated changes from the pre-industrial (PI) to recent times. As discussed by

Resources: Michel Legrand, Joseph R. McConnell, Susanne Preunkert, Andreas Stohl

Software: Andreas Plach, Andreas Stohl

Supervision: Michel Legrand

Writing – original draft: Michel Legrand, Joseph R. McConnell, Gilles Bergametti

Writing – review & editing: Michel Legrand, Joseph R. McConnell, Gilles Bergametti, Andreas Plach, Karine Desboeufs, Nathan Chellman, Susanne Preunkert, Andreas Stohl

Brahney et al. (2015), the derived budgets are very sensitive to assumptions made about the size distribution of P-containing particles. Whereas these studies consistently proposed a less than 10 μm diameter dust aerosol source of 1–2 Tg yr^{-1} (Brahney et al., 2015; Mahowald et al., 2008; Myriokefalitakis et al., 2016; Wang et al., 2015), estimates of natural emissions of primary biogenic aerosol particles (PBAP) are more uncertain, ranging from $\sim 0.16 \text{ Tg yr}^{-1}$ (Mahowald et al., 2008; Myriokefalitakis et al., 2016) to 1.0 Tg yr^{-1} (Wang et al., 2015). These studies also identified human activities such as fossil-fuel combustion that alter the atmospheric P cycle particularly in less-dusty, heavily industrialized regions, but estimates of such emissions are highly uncertain. For instance, different assumptions about gas/particle partitioning in the plume during coal combustion result in more than an order of magnitude range in P emissions (from 0.02 to 0.06 Tg yr^{-1} by Graham and Duce (1979), Mahowald et al. (2008), and Myriokefalitakis et al. (2016) to 0.6 Tg yr^{-1} by Wang et al. (2015)). Given these uncertainties, it is difficult to evaluate the importance of the different activities that have altered the atmospheric P cycle and the consequences for marine and terrestrial ecosystems.

Ice cores extracted at cold high-elevated glaciers located near industrialized regions of the northern hemisphere can help to improve understanding. To our knowledge, however, P was not yet investigated in ice cores. Here we present a seasonally resolved (1890–2000) ice-core record of P deposition extracted from the Col du Dôme (CDD) glacier located near the Mont Blanc summit. Our goal was to examine to what extent human activities have disturbed the atmospheric P budget in western Europe and to identify the underlying processes, while also investigating natural P emissions—in particular primary emissions of dust and biogenic aerosol. This is the first report of long-term observations of P concentrations and depositional fluxes extracted from a European glacial archive.

2. Materials and Methods

2.1. Ice-Core Material, Dating, and Methods

Chemical and elemental analyses were made on archived ice cores extracted from the CDD site (45.8°N, 6.8°E, 4,250 m above sea level, asl) located near the Mont Blanc summit in the French Alps. A seasonally resolved record of the 20th century P deposition in western Europe was obtained by using two ice-cores: the 126 m C10 core drilled in 1994 and the 140 m CDM core drilled less than 20 m away in 2012. The glaciological properties of the CDD site are detailed in Preunkert et al. (2000). The ice cores were dated by annual layer counting primarily using pronounced seasonal variations in ammonium (NH_4^+) concentrations (Figure 1), resulting in a composite continuous record from 1890 to 2000 (Legrand et al., 2018), with a dating error of 1 year in the upper layers and ~ 5 years prior to 1930. Because of greater wind erosion after winter snow deposition, the CDD record better documents summer deposition during the 20th century. Indeed, although winter layers can be identified back to 1890, prior to 1930 many of the winter NH_4^+ minima were too thin to determine winter means reliably so only six winter values were calculated during this period (Legrand et al., 2022).

Prior to 1890, no winter snow was preserved in the CDD ice, but the layers located between 123 and 125 m depth along the C10 core were estimated to cover time periods prior to 1850 (Text S1, Figure S1 in Supporting Information S1). To further document PI levels, additional measurements were made in the bottommost samples of a third ice-core (CDK core, 124-m long) drilled in 2004, less than 50 m from the C10 and CDM sites, for which the chronology of the basal ice was established using ^{14}C analysis of particulate organic carbon (Preunkert et al., 2019).

The chemical and elemental analyses were conducted using the continuous flow ice core system at the Desert Research Institute (DRI) Ultra Trace Chemistry Laboratory (McConnell et al., 2019). Longitudinal core samples (3.3 cm \times 3.3 cm) were melted sequentially. P and other elements including cerium (Ce) and manganese (Mn) were measured in meltwater from the innermost 10% of the sample cross-section using two inductively coupled plasma mass spectrometers operating in parallel. Ce was used here to estimate the crustal fractions of P and Mn. Mn is used here as a proxy of natural emissions of biogenic aerosol which also is a main non-crustal natural source of P (Section 4.1.2). Mn also results from steel industry emissions (see Section 4.2). Immediately after melting on an ultraclean ceramic melterhead, the meltwater stream was acidified with ultra-pure nitric acid (1% by mass). The time to transit through Teflon tubing from the melter head to injection into the HR-ICP-MS instruments was approximately 4.2 min. About 1 min prior to injection into the HR-ICP-MS instruments, a second acidification with ultra-pure nitric acid (2% by mass) was applied. As detailed in McConnell et al. (2019), with an on-line acidification of samples limited to a few minutes, the DRI

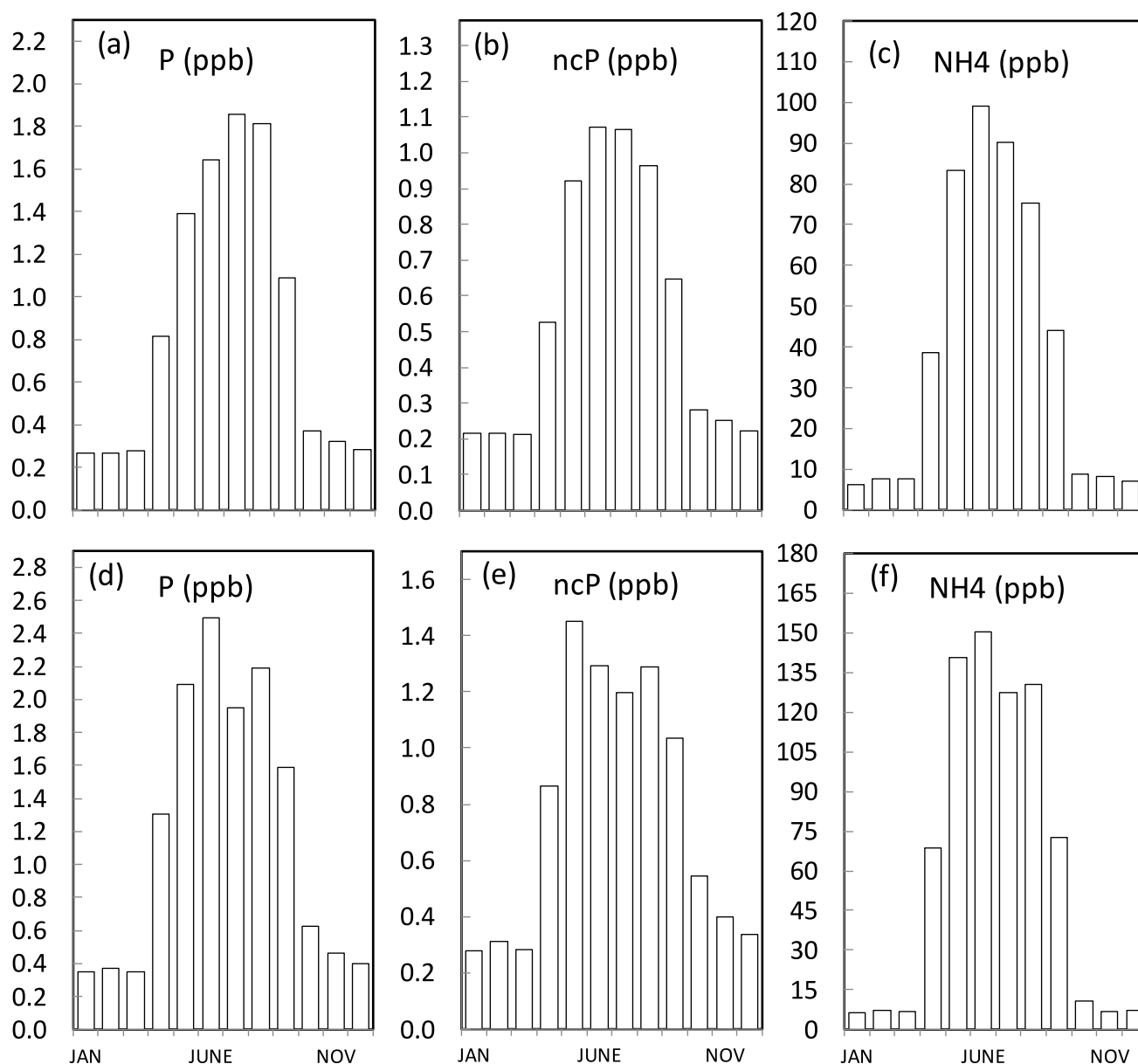


Figure 1. Mean seasonal concentrations of phosphorus (a and d) and its non-crustal fraction (ncP) (b and e), and NH_4^+ (used for seasonal dissection as detailed in Text S1 in Supporting Information S1, c and f) observed in Col du Dôme ice deposited from 1930 to 1950 (top), and from 1950 to 1985 (bottom). All concentrations are in ng g^{-1} (ppb).

system was shown to recover 100% and 60% of Pb and Ce, respectively. That is because Ce is mainly present in relatively large dust particles and so remains in the particle phase longer than other elements associated with pollution that are adsorbed onto smaller particles and so readily washed off during on-line acidification. Arienzo et al. (2019) reported a higher recovery for Mn (82%) than Ce (66%) in PI Greenland ice. Therefore, we did not correct Mn concentrations for a possible slight under-recovery of the crustal Mn fraction. This crustal fraction represented about half of the Mn in PI ice (see Section 3.3) and was only a minor component relative to the anthropogenic fraction after the PI (see Section 4.2). Although data on the recovery of P during continuous ice core analysis are not available, P likely is more soluble and less refractory than Mn so we expect an even better recovery for P. Therefore, no correction was applied to P concentrations. The detection limits were determined as three times the standard deviations of the blank (50 pg g^{-1} for P, 0.03 pg g^{-1} for Ce, and 3.0 pg g^{-1} for Mn).

2.2. FLEXPART Model Simulations

The CDD ice records were used to constrain various estimates of P emissions from nearby European countries. To account for effects of atmospheric transport and deposition, we used backward simulations with the Lagrangian particle dispersion model FLEXPART 10.4 (Pisso et al., 2019) to estimate the sensitivities of CDD dry and wet deposition to the emissions of P in Europe. With backward simulations for dry and wet deposition (Eckhardt et al., 2017), the emission sensitivity represents a source-receptor relationship that maps the sensitivity of deposition at the site (receptor) to an emission flux (source). The model was run at monthly intervals, and particles were traced backward for 30 days, which is longer than typical aerosol lifetimes in the atmosphere. Simulations were done for the period 1960 to 2000 using the ERA-5 reanalysis ($0.5^\circ \times 0.5^\circ$ resolution, 137 vertical layers of which 41 are located below 5,000 m asl) (Hersbach et al., 2020). Because commodity statistics were available only at the country scale, gridded emission sensitivities were averaged for each country and used to estimate deposition fluxes. This was done by weighting emissions from each country by its emission sensitivity and then summing to get the simulated deposition rate.

Simulated deposition rates were compared to observed deposition rates at the ice-core site as calculated by multiplying observed ice core concentrations by an assumed constant precipitation rate at the site. Present precipitation rates at the high-elevation CDD site are not monitored and information on past accumulation rates cannot be derived directly from the ice-core records because of elevation and slope-dependent wind-driven erosion (Section 2.1). However, present-day precipitation rates at CDD can be estimated using lower-elevation observations in the Mt Blanc area. Measurements at the nearby Chamonix station located at 1035 m asl record an annual precipitation rate of ~ 1.25 m with similar amounts occurring in summer and winter ([//fr.climate-data.org/europe/france/rhone-alpes/chamonix-mont-blanc-66184/](http://fr.climate-data.org/europe/france/rhone-alpes/chamonix-mont-blanc-66184/)). While a slightly higher average precipitation rate is expected at the higher elevation CDD site, variations of precipitation in the Alps show no significant trends after 1901 (Masson & Frei, 2016), so we have assumed no 20th century trends in annual or seasonal snow deposition at CDD.

Differences between deposition fluxes derived from observed ice-core concentrations and simulated by FLEXPART reflect uncertainties in past emissions (including technology-driven changes in emission factors (EFs)) and model biases, in particular overestimated deposition because of ERA5 model resolution (~ 55 km \times ~ 44 km for the CDD grid cell with the surface located at 1750 m asl). We evaluated the robustness of the FLEXPART simulations by examining the CDD ice-core record of Pb (Legrand et al., 2020) since anthropogenic Pb emissions for each country have been thoroughly investigated previously (Pacyna & Pacyna, 1999; Pacyna et al., 2009). The well-marked increase of Pb concentrations in CDD ice between 1950 and 1975, and the subsequent rapid decrease toward the late 1990s (Figure 2a) are qualitatively consistent with changes in well-documented Pb emissions from leaded gasoline that dominated the Pb anthropogenic budget at that time in Europe. To match simulated deposition fluxes at the surface of the CDD grid cell to deposition calculated from ice concentrations, a summer precipitation rate of ~ 1.5 m (instead of 0.5 m at Chamonix) is required. Since the model topography is substantially lower than the altitude of CDD, deposition fluxes were also simulated by accounting wet deposition only above the real height of CDD. A more realistic summer accumulation rate at CDD (0.8 m) is required to fit the observed deposition with the simulated deposition at the actual elevation of the CDD site (4,450 m asl, i.e., 2700 m above the model surface) (Figure 2b). We used this relationship between Pb ice-concentrations and simulated FLEXPART deposition fluxes simulated at the actual elevation of CDD to evaluate the quality of estimated emissions of chemical species such as P for which emissions generally are far less constrained.

Since the expected size distribution of P-containing aerosol is dependent on emission processes (e.g., submicron aerosols from fossil-fuel burning and pig-iron production vs. super-micron aerosols from PBAP), the FLEXPART simulations included submicron sulfate, black carbon (BC), and 5 μ m dust diameter aerosol for the 1960–2000 years. Figure S2 in Supporting Information S1 shows the maps of average summer emission sensitivities of the CDD site to emissions of sulfate and 5 μ m diameter dust aerosol. The emission sensitivities for countries surrounding the CDD site are enhanced for 5 μ m diameter dust aerosol compared to sulfate, reflecting more efficient deposition of large particles (dry deposition) emitted nearby and the longer atmospheric lifetimes of much smaller sulfate particles. We also tested the sensitivity of results to the size of various types of super-micron aerosols from PBAP (5 μ m spores and 30 μ m pollens) (Table S1 in Supporting Information S1).

2.3. Past Anthropogenic Emissions From Coal Burning and Pig Iron Production

Combustion of fossil-fuels (particularly coal burning) and pig iron production are thought to represent major anthropogenic sources of P (Graham & Duce, 1979; Mahowald et al., 2008; Myriokefalitakis et al., 2016; Wang

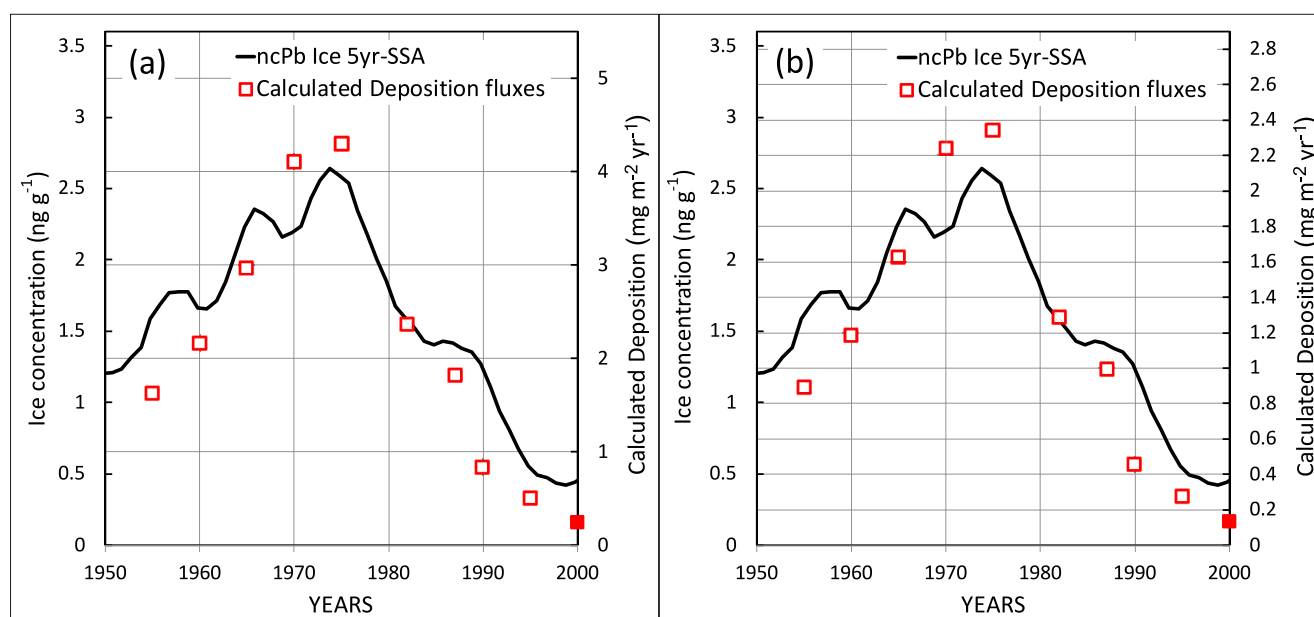


Figure 2. Summer trends of non-crustal Pb ice-concentrations (black line: first component of singular spectrum analysis with a 5-year time window, adapted from Legrand et al. (2020)) and deposition fluxes at Col du Dôme (CDD) simulated by FLEXPART using Pb emissions calculated for each country by Pacyna and Pacyna (1999) between 1955 and the 1990s (open red squares) and Pacyna et al. (2009) for 2000 (solid red square). Panels (a) and (b) refer to simulated depositions at the model surface and at the real elevation of the CDD site, respectively. The righthand scales (calculated deposition) were chosen to match trends in the ice-core concentrations and calculated deposition fluxes.

et al., 2015). To evaluate their contribution to past changes of non-crustal P (ncP) in CDD summer ice, we used coal consumption statistics from Mitchell (1975) for the period prior to 1975, and from British Petroleum (British Petroleum, 2020) for 1975–2000. For pig iron production, we used statistical data from Mitchell (1975) prior to 1975 and the U. S. Geological Survey (n.d.) for the more recent years. Focusing on summer changes, we assumed that emissions from coal burning were twice as high during the winter heating season compared to summer in most European countries (except in Southern Europe) (Fagerli et al., 2007), whereas we assumed that emissions from pig iron were constant throughout the year. Unlike toxic metals such as Pb or Cd, EFs have not been reported for P in Europe. The U.S. EPA (1973) estimated a coal burning EF for P of $\sim 8.8 \text{ g t}^{-1}$ in the late 1960s. Considering this value and accounting for EF changes in Europe from the progressive installation of electrostatic precipitators and filters in the late 1970s, as well as initial flue gas desulphurization installations in the mid-1980s, we scaled the U.S. EPA EF value based on changes of EFs for Pb from coal burning in Europe (Table 1). Using a 1968 EF for U.S. pig iron production of $\sim 11.4 \text{ g P t}^{-1}$, we applied a similar approach to the estimate European pig iron P emissions. Given the fast changes of EFs for pig iron between 1970 and 1980, we assumed that EF reductions from pollution control devices started some 10 years earlier in the U.S. than in Europe.

Table 1
Estimated Emission Factors (EFs) of Phosphorus for Coal Burning and Pig Iron Production in Europe From the 1950s to the 1990s Based on Those Proposed by Pacyna (1991) for Pb

EFs	1950	1960	1970	1980	1985	1995	References
Coal Pb	11.7	10.4	8.4	7.7	7.7	3.8	Pacyna (1991)
Coal P	12.3	10.9	8.8 ^a	8.1	8.1	4.0	See text
Pig Iron Pb	74.7	74.7	74.7	18.7	11.2	2	Pacyna (1991)
Pig Iron P	45.5	45.5	45.5	11.4 ^a	6.8	1.2	See text

Note. All EF values are in g of species emitted per t of material produced (or t of coal burned).

^aValues estimated in EPA (1973) (see text).

3. Data Presentation

3.1. Summer and Winter CDD Ice Record

Long-term chemical records extracted from alpine sites such as CDD may be affected by systematic changes in seasonal snow deposition upstream the drill site, potentially leading to pronounced trends in annual average concentrations in the ice that do not reflect atmospheric trends (Preunkert et al., 2000). Flow thinning and wind erosion upstream of the CDD drill site result in marked decreases in the annual ice layer thickness from 1.6 m water equivalent (mwe) between 1970 and 2000 to 0.46 mwe between 1930 and 1950 (see Figure S3 in Legrand et al. (2018)). Furthermore, winter layer thicknesses decrease by a factor of five between 1970–2000 and 1930–1950, while summer layers decrease by only a factor of three—with the difference

caused by progressively more preferential winter erosion upstream of the coring site. Because most chemical species exhibit pronounced differences in winter and summer concentrations (Figure 1), the result is a strong non-atmospheric trend in annual average concentrations. As done in previous CDD ice studies, here we examine summer and winter trends separately. We focus on summer trends since these ice records are more complete (see Section 2.1) and only briefly discuss winter data that are mainly available in snow deposited after 1930.

In addition to an overall increase of P concentrations over the 20th century, the CDD records show significant year-to-year variability (Figure 3). Previous atmospheric transport-chemistry simulations have shown that NH_4^+ concentrations at CDD are modulated within a factor of 2–3 by the meteorological variability (Fagerli et al., 2007). This also was the case for P with high values in 1928, 1958, 1989, and 2000, and low values in 1968 and 1978 (Figure S3 in Supporting Information S1). In some cases, however, high P values did not coincide with high NH_4^+ values (in 1970 and 1992, for instance), suggesting that, in addition to the intensity of atmospheric vertical transport, the strength of P emissions varies from year-to-year (see Section 4.1.2). To minimize this inter-annual variability on the long-term trends, we smoothed the summer ice record using the first component of singular spectrum analysis with a 7-year time window (Figure 3).

3.2. Estimation of the Crustal Fraction of P

Phosphorus and many other metals are emitted to the atmosphere as part of terrigenous particles or dust. Given the importance of dust emissions on the atmospheric P budget suggested by previous studies (e.g., Mahowald et al., 2008; Myriokefalitakis et al., 2016), an accurate assessment and removal of the crustal fraction of P present in alpine ice is required prior evaluation of past changes in natural non-crustal and anthropogenic emissions over western Europe. This is especially relevant here because a previous study of CDD ice showed significant increases in Ce concentrations during recent decades, with the rock-forming element Ce used here and in other studies as a tracer of crustal dust (Arienzo et al., 2021). This increasing recent trend is consistent with several other studies of dust in alpine ice (De Angelis & Gaudichet, 1991; Preunkert & Legrand, 2013).

The P/Ce ratio in dust particles varies with provenance so it may be inappropriate to use a global ratio (e.g., “mean sediment” from Bowen (1966)). Here we used P and Ce concentrations in CDD ice to determine a site-specific P/Ce ratio (Figure S4 in Supporting Information S1), as done in previous CDD ice-core studies (Arienzo et al., 2021; Legrand et al., 2020). This approach suggested a site-specific crustal P/Ce ratio of 11.1 after accounting for an under-recovery of 1.66 resulting from the continuous analysis at DRI. This compares to 8.1 reported for “mean sediment” (Bowen, 1966) (Text S2 in Supporting Information S1). This site-specific P/Ce ratio (11.1) and the under-recovery corrected measured Ce concentrations were used to estimate and remove the crustal P from the total measured P to yield ncP.

3.3. The Pre-Industrial Levels

Prior to 1890 (i.e., below 118.3 m depth), the continuous analyses indicated that no winter snow was preserved, thereby precluding dating by annual layer counting but allowing evaluation of summer-dominated concentrations prior to industrialization and significant emissions from coal burning and industrial processes. Here we focus on the CDD record from 118 to 125 m depth. Although the exact dating is uncertain (Text S1 in Supporting Information S1), all evidence suggests that ice from 123 to 125 m was deposited prior to 1850 (Figure S1 in Supporting Information S1).

4. Result and Discussions

Prior to 1850 (Table 2), summer P concentrations in CDD ice were $\sim 0.9 \text{ ng g}^{-1}$. Concentrations slightly exceeded 1 ng g^{-1} during the early 20th century but then increased markedly after 1950, reaching $\sim 2.5 \text{ ng g}^{-1}$ over the 1990s, so enhancement of only 2.5 above PI levels (Figure 3). Although the increases are clear, P is unusual since most trace element species measured in CDD ice show far greater changes. For example, cadmium and zinc concentrations (Legrand et al., 2020), vanadium and molybdenum (Arienzo et al., 2021), and thallium (Legrand et al., 2022) all increased by more than a factor of 10. However, all of these pollutants were dominated by fossil-fuel burning and industrial emissions, suggesting relatively significant natural or background sources of P.

The increase of total P concentrations from PI (0.9 ng g^{-1}) to PD (2.5 ng g^{-1}) was due partly to an increase of the crustal fraction (from 0.36 ng g^{-1} to 1.1 ng g^{-1}) but also to an increase in the non-crustal fraction from 0.56 ng g^{-1}

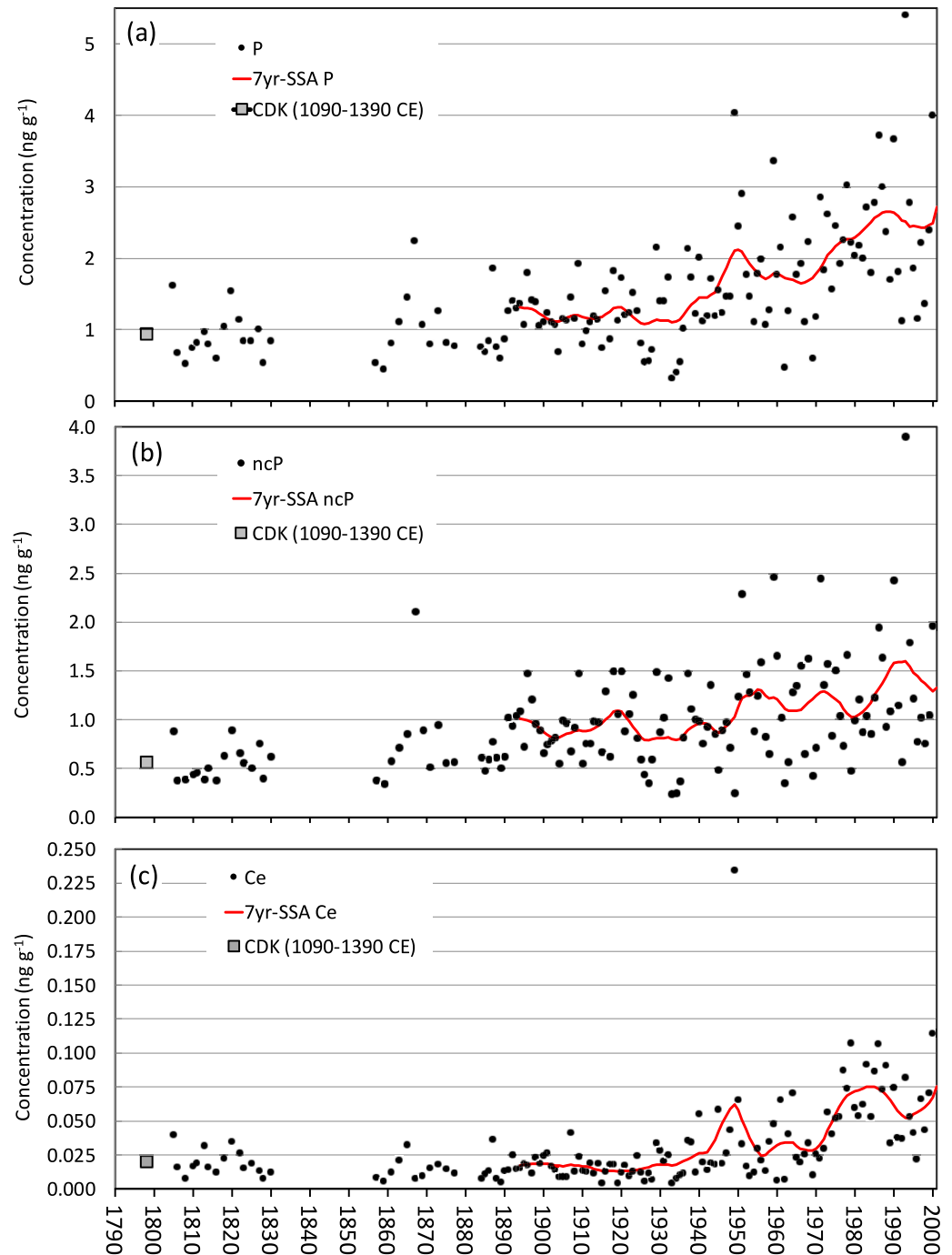


Figure 3. Long-term Col du Dôme ice-core trend in summer of P (a), non-crystal P (b), and Ce (c) (not corrected from the under-recovery, Section 2.1). The gray squares on the left are values observed in CDK ice (1090–1390 common Era, see Section 2.1 and Table 2). The red lines are first component of singular spectrum analysis with a 7-year time window. Note the large Ce value observed in 1949 (0.234 ng g^{-1}).

during the PI to 1.4 ng g^{-1} during the PD. In the following, we discuss the natural sources of P (crystal and non-crystal) that contribute to the PI level of P in alpine ice, and the likely causes of the increase of non-crystal sources that led to the observed increase of total P levels.

Table 2
Pre-1890 Concentrations (Mean \pm σ) of Phosphorus and Manganese and Their Non-Crustal Fractions (ncP and ncMn) Along With Ce Concentrations (Not-Corrected From the Under-Recovery, See Section 2.1)

Years CE	P	Mn	Ce	NH ₄	ncP	ncMn
1884–1893	1.03 \pm 0.41	0.58 \pm 0.27	0.015 \pm 0.009	47 \pm 15	0.72 \pm 0.21 (70%)	0.35 \pm 0.07 (60%)
1857–1877	1.03 \pm 0.50	0.52 \pm 0.19	0.014 \pm 0.008	40 \pm 7	0.77 \pm 0.05	0.33 \pm 0.14
	0.91 \pm 0.32 ^a	0.49 \pm 0.18 ^a	0.015 \pm 0.008 ^a	39 \pm 7 ^a	0.63 \pm 0.21 ^a (69%) ^a	0.29 \pm 0.09 ^a (59%)
1805–1835	0.91 \pm 0.31	0.49 \pm 0.19	0.019 \pm 0.009	51 \pm 21	0.55 \pm 0.17 (60%)	0.24 \pm 0.09 (49%)
1090–1390 ^b	0.94 \pm 0.33	0.49 \pm 0.08	0.020 \pm 0.008	64 \pm 13	0.57 \pm 0.32 (60%)	0.22 \pm 0.10 (49%)

Note. For ncP and ncMn, we reported under parenthesis their mean contributions to the total. All concentrations are in ng g⁻¹.

^aExcluding the high outlier in ~1867 (Section 4.1.2). ^bFrom the CDK ice core (Section 2.1).

4.1. Natural Sources of Phosphorus in Western Europe

4.1.1. Crustal Phosphorus Emissions and Their Changes Over the Past

Around a third of the P levels in PI summer ice is of crustal origin (Table 2). The increase of P deposition in alpine summer ice was partly due to an increase of 0.74 ng g⁻¹ of its crustal fraction, particularly during the second half of the 20th century, as indicated by the Ce increase from ~0.017 ng g⁻¹ during the PI to 0.057 ng g⁻¹ after 1980 (Figure 3). Note that use of the P/Ce ratio in mean sediments (see Section 3.2) would have led to an overestimation of the increase of the ncP fraction (0.9 ng g⁻¹ instead of 0.7 ng g⁻¹, Figure S5 in Supporting Information S1).

Using mineralogical observations, De Angelis and Gaudichet (1991) concluded that a 10-fold increase in Al deposition from 1955 to 1967 to 1983–1985 measured in a 1986 CDD ice-core was due to greater long-range transport of Saharan dust. Though limited to 18 years of measurements, the 1984–2001 measurements of Saharan dust deposition in Corsica (Mediterranean Sea) (Figure 4a) also showed a maximum in the 1980s followed by a strong decrease in the 1990s (except in 1993) (Desboeufs et al., 2018; Loÿe-Pilot & Martin, 1996). These findings are consistent with recent changes in Ce in the 1994 and 2012 CDD ice cores (Figure 4b) when considering inherent ice-core dating uncertainties.

Data from the 1986 CDD ice core and the dust deposition record in Corsica pointed the early 1970s and the early 1990s as periods of low Saharan dust input over the Mediterranean Sea and further north over the Alps. Over these years, the Ce ice record indicates a concentration of 0.02 ng g⁻¹ in the earlier 1970s and of 0.04 ng g⁻¹ in 1991–1992 (Figure 4b). If confirmed, the CDD Ce record suggests that during the second half of the 20th century, a non-Saharan dust source significantly contributed to Ce levels in the Alps and that this source may have doubled from the 1970s to the 1990s, possibly as a result of human-influenced land use changes in western Europe.

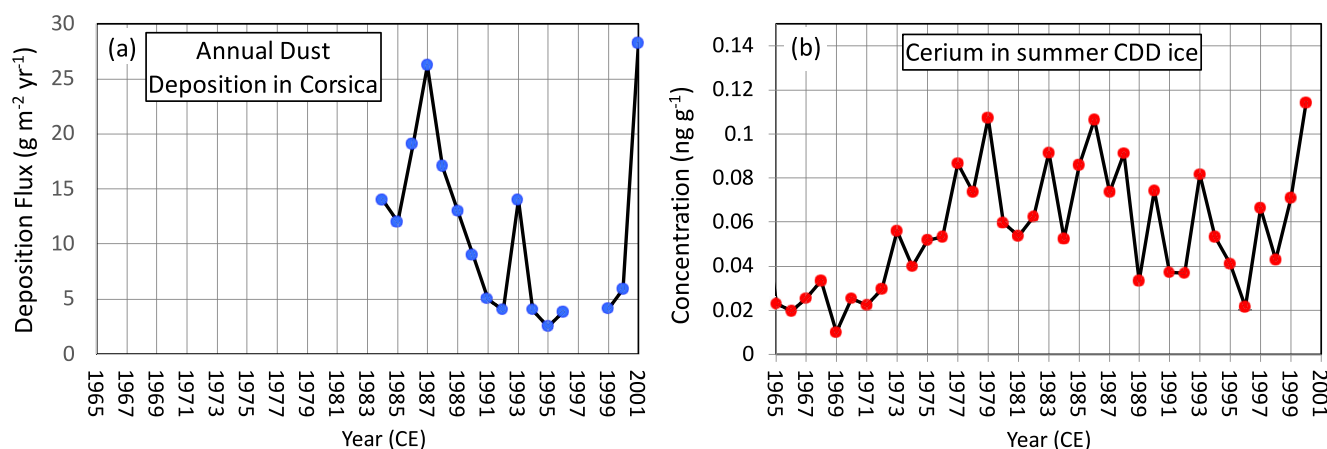


Figure 4. Recent changes of crustal deposition in Europe. (a) Annual Saharan dust deposition in Corsica between 1984 and 2001 (adapted from Desboeufs et al. (2018)). (b) Ce (not corrected for the under-recovery, Section 2.1) deposition in summer Col du Dôme ice over the recent years.

4.1.2. Non-Crustal Emissions: Importance of PBAP Over Western Europe

CDD ice-core data revealed the occurrence of a significant natural non-crustal source of P in the western European atmosphere in summer. In addition to dust emissions, P is emitted naturally from volcanoes, sea spray, biogenic processes, and natural biomass burning (e.g., Graham & Duce, 1979).

Volcanoes emit various trace elements including P for which far few observations are available compared to metals such as Pb, or Zn. Sicily's Mount Etna continuously emits large amounts of metals (Calabrese et al., 2011), including from 77 to 840 t of P per day as a result of quiescent degassing (Bergametti et al., 1984). Using the FLEXPART emission sensitivity for Sicily of $400 (\mu\text{g m}^{-2} \text{ yr}^{-1})/(\text{kg s}^{-1})$ (Figure S2a in Supporting Information S1), the estimated P deposition fluxes at CDD related to continuous Etna emissions would be $0.5\text{--}5.0 \mu\text{g m}^{-2}$ corresponding to a summer ice concentration of $7 \cdot 10^{-4}$ to $7 \cdot 10^{-3} \text{ ng g}^{-1}$, far lower than the PI level of 0.56 ng g^{-1} . Although based on limited data, this rough calculation suggests that Etna emissions remain a minor contribution to the P budget in western Europe.

P is present in the marine biosphere and is emitted along with sea-salt aerosol. This source, however, would be minor at high-elevation alpine sites. Legrand et al. (2002) reported mean summer Na levels in CDD ice of 15 ng g^{-1} of which less than 7 ng g^{-1} was attributed to sea-salt. Using an enriched P/Na ratio of $2 \cdot 10^{-4}$ instead of $5.6 \cdot 10^{-6}$ in seawater (Graham et al., 1979; Pilson, 1998), we estimate a marine P contribution of $\sim 1.4 \cdot 10^{-3} \text{ ng g}^{-1}$ which again is far below the PI value of 0.56 ng g^{-1} .

At the global scale, biomass burning is a source of P, with estimates ranging from 18 kt yr^{-1} (Myriokefalitakis et al., 2016) to 800 kt yr^{-1} (Wang et al., 2015). Using a mean emission rate of $3 \cdot 10^{-4} \text{ ng m}^{-2} \text{ s}^{-1}$ in western Europe (Figure S1 from Myriokefalitakis et al. (2016)) primarily during summer and emissions sensitivities calculated by FLEXPART for BC aerosol, we calculate a mean summer deposition rate at CDD of $0.63 \mu\text{g m}^{-2}$ equivalent to a biomass burning contribution to P concentrations of $8 \cdot 10^{-4} \text{ ng g}^{-1}$.

Although highly uncertain, emissions of PBAP that consist of structural units (e.g., pollen, spores, and bacteria) and fractionated material (plant debris) (see Després et al. (2012) for a review) are considered to be the main natural ncP source. Among the many trace species that were investigated in CDD ice, Mn is the only element whose non-crustal natural emissions generally exceed a few tens of kt yr^{-1} (mean value of 96 kt yr^{-1}) of which 27 kt yr^{-1} are emitted as PBAP (Nriagu, 1989). In CDD ice, the PI level of ncP (0.56 ng g^{-1}) is higher than ncMn (0.23 ng g^{-1} , Table 1). Although measurements of Mn and P contents in various bioaerosols are sparse, this is consistent with a larger abundance of P in vegetation (Garivait et al., 1996, 1997; Guha & Mitchell, 1966) and pollens (Taha & Al-Kahtani, 2020). The strong covariance of ncP and ncMn observed in PI summer ice (Figure 5a) supports the contention that PBAP emissions are the dominant sources of ncP and ncMn over western Europe in summer. Note that the observed high (low) ncP concentrations did not coincide with high (low) NH_4 levels (Figure 5b). For instance, the highest (2.1 ng g^{-1}) and the lowest (0.38 ng g^{-1}) ncP values occurred in ice layers with similar NH_4 levels ($\sim 46 \text{ ng g}^{-1}$), suggesting that the observed year-to-year variability in ice concentrations was related to changes in PBAP emissions rather than inter-annual variability of the upward transport since high NH_4 values at CDD have been linked to enhanced upward transport from the boundary layer.

In the following, we used ncP levels observed in CDD ice that we attribute to PBAP emissions to constrain prior estimates of this source ranging from 0.16 to 1.0 TgP yr^{-1} (Myriokefalitakis et al., 2016; Wang et al., 2015) for present-day. This large range in the PBAP source estimates of P are related to uncertainties in that amount of emitted PBAP and the assumed P content of biogenic particles. For example, assuming a global PBAP emission of 50 TgC yr^{-1} that mainly consists of $\sim 5 \mu\text{m}$ fungal spores (40%) and $\sim 30 \mu\text{m}$ pollen grains (60%) (Hoose et al., 2010), and a mean P/C mass ratio of $2.5 \cdot 10^{-3}$ (range of $0.015\text{--}0.00015$), Kanakidou et al. (2012) and Myriokefalitakis et al. (2016) calculated a PBAP emission of $0.156 \text{ TgP yr}^{-1}$. Wang et al. (2015) proposed a value up to 1 TgP yr^{-1} considering a far larger PBAP emission rate (1000 Tg yr^{-1} , Jaenicke, 2005). Considering a PBAP emission of $0.02\text{--}0.03 \text{ ng m}^{-2} \text{ s}^{-1}$ in western Europe (Figure S1 from Myriokefalitakis et al. (2016)) mainly during summer would lead to a P emission of 0.01 and $0.015 \text{ ng m}^{-2} \text{ s}^{-1}$ for spores and pollens, respectively. Using FLEXPART simulations, we calculated the corresponding deposition of P at CDD. As seen in Table S1 and S2 in Supporting Information S1, emissions sensitivities of France and Italy indicate that these two countries are the dominant contributors to the deposition of super-micron particles at CDD, well before Spain and Germany. The contribution of spores to deposition of P at CDD was estimated by using emissions sensitivities calculated by FLEXPART for $5 \mu\text{m}$ dust diameter aerosol (Figure S2 in Supporting Information S1) that were corrected by a

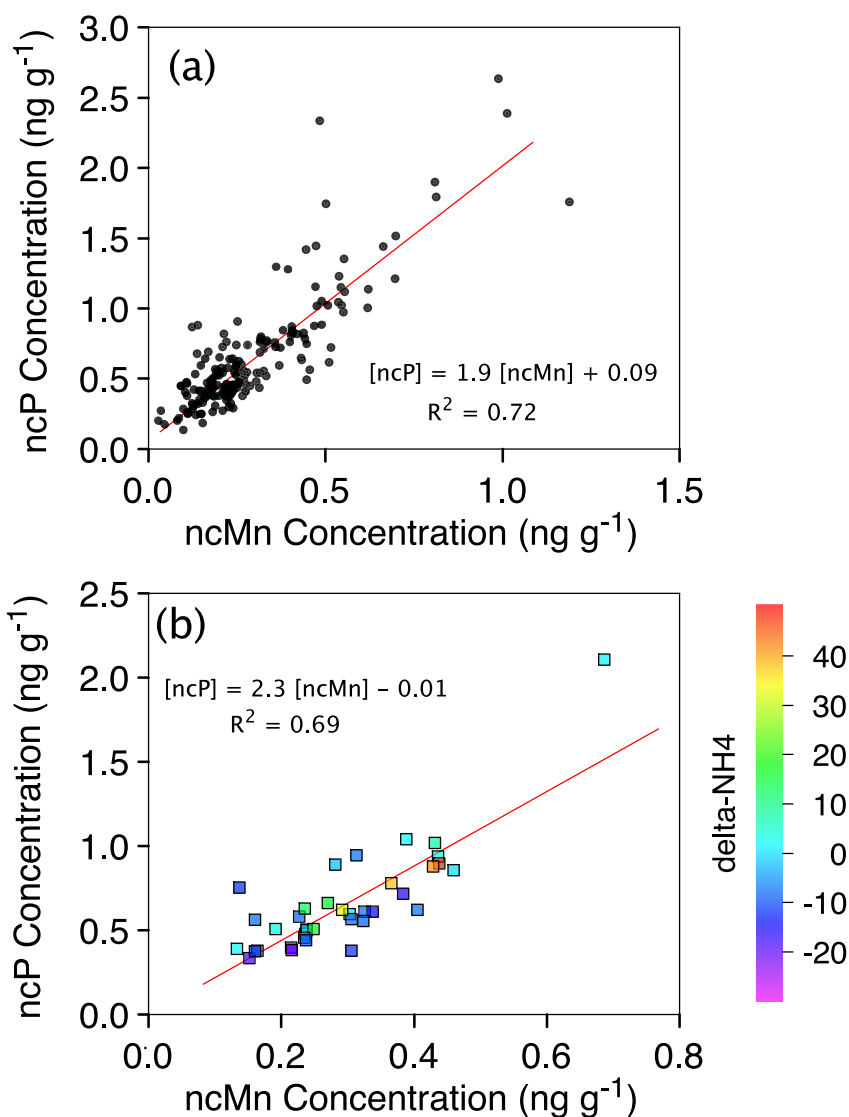


Figure 5. Relationship between non-crustal fraction of P and Mn (non-crustal P (ncP) and ncMn) in pre-industrial (PI) summer Col du Dôme (CDD) ice. (a) Raw data, (b) annual values. For annual values, colors indicate the deviation of NH_4^+ concentrations in individual mean summer values (ΔNH_4^+) with respect to the mean NH_4^+ concentrations observed in PI ice deposited at CDD. The ice layer exhibiting the highest ncP and ncMn levels is dated to 1867.

factor of ~ 0.6 to account for the lower density of PBAP ($d = 1$, Hoose et al., 2010) than the one that was assumed for dust particle ($d = 2.6$) (see Table S2 in Supporting Information S1). Table S1 in Supporting Information S1 shows that the emissions sensitivities from France and Italy are three times higher for $30 \mu\text{m}$ particles than for $5 \mu\text{m}$ particles. This factor was applied to emissions sensitivities calculated by FLEXPART for $5 \mu\text{m}$ diameter aerosol to calculate the deposition of P related to pollens. The resulting deposition of P related to PBAP reached $0.14 \text{ mg m}^{-2} \text{ yr}^{-1}$ for spores and $0.55 \text{ mg m}^{-2} \text{ yr}^{-1}$ for pollens. Referring to Figure 2b, this would imply a ncP ice concentration of 0.85 ng g^{-1} compared to a 0.56 ng g^{-1} in PI ice and to a 1.1 ng g^{-1} in PD ice when considering the recent increase of PBAP in France after 1970 (see further discussions in Section 4.2). These rough estimates are consistent with the lower range of estimated PBAP emissions at the global scale ($0.156 \text{ TgP yr}^{-1}$). The slightly difference by less than a factor of 2 between observed and calculated present-day deposition fluxes may be due to omission of emissions of very coarse pollens and vegetation debris that were not considered in the emission of $0.03 \text{ ng m}^{-2} \text{ s}^{-1}$ for western Europe (Myriokefalitakis et al. (2016)).

Omission of vegetation debris is not necessarily legitimate. Indeed, measurements of cellulose (Puxbaum & Kunit, 2003), a good proxy of plant debris, indicated its significant presence in particles of less than $1.6 \mu\text{m}$,

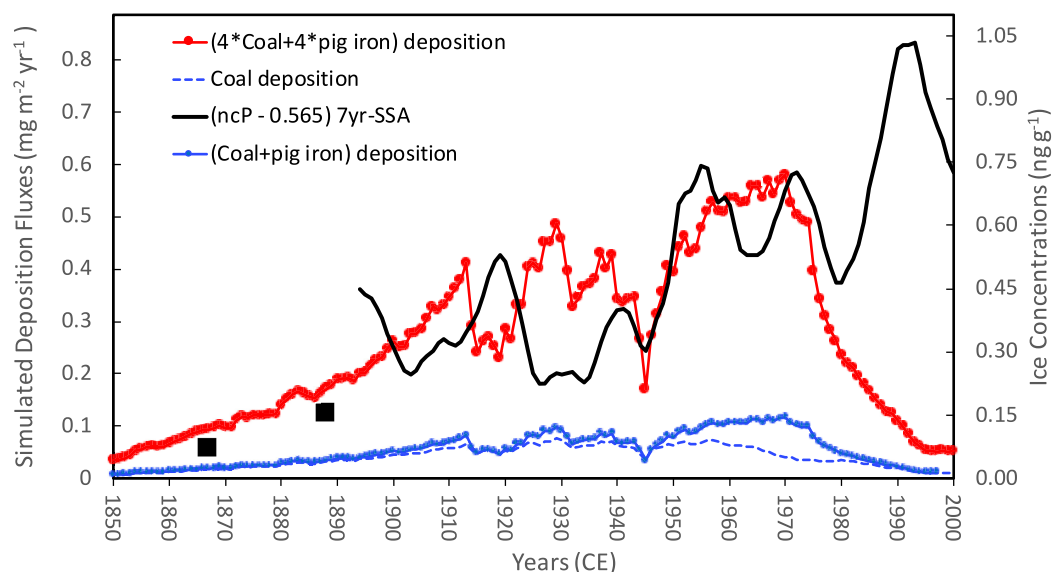


Figure 6. Summer ice-core trends of non-crustal P concentrations (black line: 7yr-SSA) from which the pre-industrial value of 0.56 ng g^{-1} (Table 2) was subtracted, and deposition fluxes at Col du Dôme calculated by FLEXPART using estimated past anthropogenic emissions from coal burning (blue dashed line) and coal burning plus pig iron production (blue dots). The red line represents deposition fluxes calculated when multiplying emissions from both coal-burning and pig-iron production by a factor of 4 (see text). Black squares denotes mean concentrations observed in summer ice deposited prior to 1890 (Table 2). The scaling between ice concentrations and simulated deposition fluxes is the same as in Figure 2b.

accounting for 43% of total mass of particles of less than $25 \mu\text{m}$. Furthermore, the relatively high ncP winter values in ice compared to anthropogenic species (Figure 1) are consistent with atmospheric cellulose levels observed at high elevation in the Alps (Sánchez-Ochoa et al., 2007), suggesting emissions from well above the boundary layer (e.g., from vegetation located up to 2,000 m asl in alpine regions).

4.2. Causes of ncP Increase Over the 20th Century: Role of Fossil-Fuel Combustion

ncP at CDD had increased above PI levels by the early 20th century. This was followed by a plateau until 1950. A second increase of similar magnitude occurred soon after 1950 and persisted until the end of the 20th century. The mean PI concentration (0.56 ng g^{-1} , Table 2) increased to 0.63 ng g^{-1} in the 1860–1870 and further to 0.72 ng g^{-1} in the 1890s, to reach a first plateau at 0.90 ng g^{-1} from 1890 to 1950 and a second one at 1.28 ng g^{-1} from 1950 to 2000 (Figure 3).

To evaluate the importance of emissions from coal burning and pig iron production, we calculated deposition fluxes at CDD using emission sensitivities simulated by FLEXPART and emissions estimated from pig iron production and coal consumption commodity statistics after incorporating the estimated EFs values reported in Table 1 (Section 2.3). The agreement between simulated deposition and observed ice concentrations is not perfect, but the overall ncP trend in ice characterized by an increase starting prior to 1900 and reaching a maximum during the second part of the 20th century (Figure 6) is qualitatively well reproduced by FLEXPART-based estimates, except over the last two decades of the 20th century. The significant departure between observed and simulated deposition observed prior to 1950 may be due either to dating errors that can be as much as 5 years during that period of the ice-core records (Section 2.1) or to the poor quality of commodity statistics during World War I and II. Assuming a similar relationship between simulated and observed Pb concentrations (Figure 2b), the simulated P depositional are about four times higher than expected. The lack of EF data hinders identification of the causes. For instance, in a review of P content in coal, Swaine (1990) stated “in the absence of sufficient data, it is difficult to assess a range for P content perhaps from 10 to 3,000 ppm.” As a result, we cannot assess differences in P content of European and U.S. coal.

Probably more important is that the EFs for combustion processes (coal and pig-iron) used here to calculate deposition at CDD were based on the P content of ash without including gaseous P emissions. Similarly, global

emissions from coal burning from Mahowald et al. (2008) and Myriokefalitakis et al. (2016) were based on BC inventories and estimated P/BC values during combustion also without considering gaseous P emissions. Though the mass balance of P during combustion is not available, assuming that during combustion a large P fraction is emitted in the gas phase (i.e., phosphorus oxides) that subsequently condense on background atmospheric aerosols, Wang et al. (2015) derived a combustion P source that is 20-fold higher than the other estimates. A very recent study of the P mass balance during coal combustion in household stoves suggested that gaseous emissions are double particulate emissions in the residential sector (Xu et al., 2023). While this study indicated that gaseous P emissions cannot be ignored, it did not support the factor of 20 proposed by Wang et al. (2015). The discrepancy by a factor of 4 between observed and calculated deposition fluxes at CDD (Figure 6), may be attributed to an underestimate of emissions calculated on the basis of P content of ash or P/BC without considering gaseous emissions. Conversely, assuming an annual P emission from fossil-fuel combustion in 1960 of $10 \text{ mg m}^{-2} \text{ yr}^{-1}$ in France (Figure S2 in Wang et al., 2015), during a period when coal dominated fossil-fuel consumption, we calculated an annual source of 5 kt of P. Assuming a corresponding summer emission of $\sim 1.65 \text{ kt}$, the FLEXPART-simulated summer deposition flux would be $1.4 \text{ mg m}^{-2} \text{ yr}^{-1}$ due to French coal-burning. Assuming that deposition resulting from emissions from other western European countries, we obtained a FLEXPART-simulated deposition fluxes corresponding to 3.5 ng g^{-1} of ncP (i.e., 6 times higher than the ncP increase from PI to 1960, Figure 3). Consequently, the CDD ice records suggest that the lower previous estimates of P emissions from coal burning P emissions for western Europe were too low using either the P/BC ratio or EFs estimated from the P content of ash, whereas the upper range obtained assuming a large release in the gaseous P probably overestimated emissions by a factor of 6.

Finally, in addition to combustion, the fertilizer industry and fertilizer applications emit phosphates to the atmosphere. Fertilizer EFs have been estimated for the U.S. (EPA, 1973), but a major hindrance to quantifying this contribution is that the particle size distribution of the emissions is unknown. European fertilizer production that was dominated by France reached a maximum of 2 Mt yr^{-1} in the 1920s (Figure S7 in Supporting Information S1). CDD ice-core data (Figure 3) show no evidence of a P increase at that time, suggesting that this industry represented an insignificant P source at CDD. The same is true for phosphate applications that reached a maximum of 0.9 Mt of P yr^{-1} in 1980 instead of 0.45 Mt of P yr^{-1} in the mid-1990s in France (Boulaïne, 1995).

During the two last decades of the 20th century, the ice-core data and estimated deposition fluxes did not agree with the expected large decrease of emissions from coal burning and pig iron production resulting from both decreased consumption (production) as well as lower EFs following recent efforts to reduce emissions. Though the EF decreases after 1970 are crude estimates, the CDD ice-core records of ncTl and ncMn (Figure S6 in Supporting Information S1), pollutants also mainly emitted by coal burning (Legrand et al., 2022) and the steel industry (Legrand et al., 2023a, 2023b), respectively, are consistent with strong emissions reductions. The absence of recent ncP decrease suggests emissions from another anthropogenic source. A likely candidate might be growing biofuel emissions but growth started only at the beginning of the 21st century in Western Europe. If not related to an unknown anthropogenic source, the excess of ncP (in the order of 0.6 ng g^{-1}) with respect to simulated deposition fluxes (Figure 6) may be related to recent land-use changes that led to enhanced PBAP emissions. PBAP emissions of fungal spores probably increased strongly following a late 20th-century expansion of forested areas in France. This expansion was particularly pronounced from 1960 to 1980 (Figure 7) but the departure between anthropogenic ncP concentrations observed in the ice (black line in Figure 6) and estimated contribution of emissions from coal burning and pig iron (red line in Figure 6) was larger only after 1980. Such a time lag may be the result of the time required for trees to reach maturity. Furthermore, the increases of forested area were larger after 1980 in south/south-east French regions (<https://inventaire-forestier.ign.fr/IMG/pdf/IF31.pdf>). The higher emissions sensitivities for these regions (Figure S2 in Supporting Information S1) suggest that emissions from these post-1980 increases in forested area may have had an especially large impact on the CDD record. Finally, increasing air temperatures and decreased snow cover duration enabled development of high-elevation plant communities and plant colonization of habitats previously characterized by long-lasting snow cover. Such a recent increase of plant cover in alpine valleys, the “greening” trend, is clearly revealed by 30 years of satellite observations (Carlson et al., 2017), particularly from 1980 to 1990. It therefore seems likely that PBAP emissions that accounted for 0.6 ng g^{-1} of ncP levels during PI increased during recent decades, significantly counteracting decreasing P emissions from coal burning and pig iron production after 1975.

As summarized in Table 3, whereas most of the increase of P from 1900 to 1950 is attributed to coal burning, the further increase observed between 1950 and 1975 probably was the result of emissions from the pig iron industry

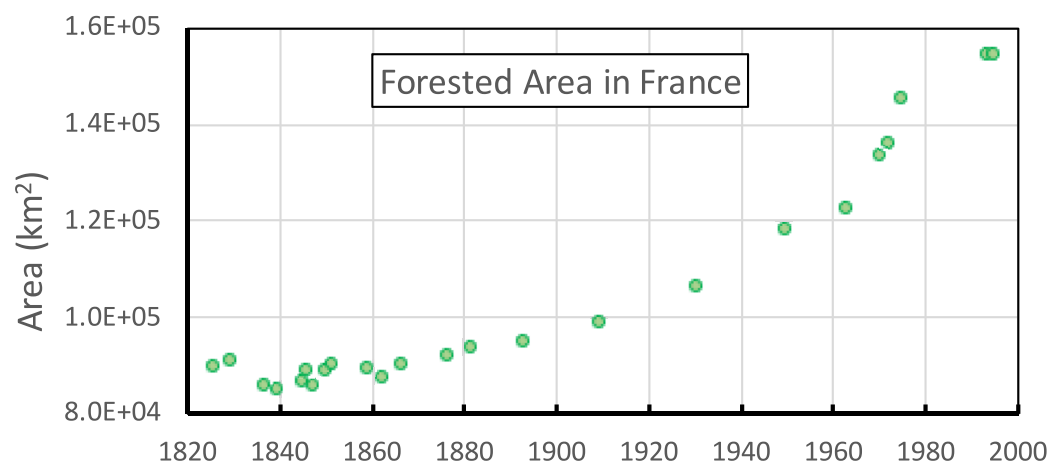


Figure 7. Change of the forested area in France since 1820 (Cinotti, 1996).

together with a possible slight increase of PBAP following an increase of forested areas in France (Figure 3). Finally, although industrial P emissions declined during the two last decades of the 20th century, P concentrations at CDD increased. We attribute the increased P to enhanced dust deposition in the Alps and a further increase of the PBAP source.

5. Conclusions

This study is the first investigation of P concentrations in ice extracted from a cold glacier located in the mid-latitudes. About two thirds of the total P measured in summer ice during the PI can be attributed to primary biogenic emissions and the remainder to crustal dust sources. The more than doubling of total P in the CDD records by the 1990s partly was the result of increased dust deposition particularly during the second half of the 20th century, but ncP increases prior to ~1980 are consistent with increasing emissions from coal burning and pig iron production. The absence of post-1980 decrease of P deposition in CDD ice, despite reduced emissions from fossil fuel combustion and industrial processes documented by other pollution tracers, implies enhanced biogenic emissions possibly linked to large extensions of forested areas in France and possibly the greening trend in high alpine valleys. The CDD records suggest global-scale P emissions from coal burning of 0.16 Tg yr⁻¹, compared with previous estimates ranging from 0.04 to 1 Tg yr⁻¹, and primary biogenic emissions of 0.16 Tg yr⁻¹ which is in the lower range of prior global estimates. Reduced uncertainties are particularly important for ecosystem studies since P in coal burning and primary biogenic emissions consists of soluble, largely bioavailable phosphorous.

Table 3
Apportionment of the Different Natural and Anthropogenic Sources to P Concentrations Observed in Col du Dôme Summer Ice Deposited From Pre-Industrial (PI) to the 1900–1950 Time Period, From 1950 to 1975, and 1975 to 2000

	PI	1900–1950	1950–1975	1975–2000
P	0.93 ng g ⁻¹	1.30 ng g ⁻¹	1.8 ng g ⁻¹	2.5 ng g ⁻¹
Crustal	0.36 ng g ⁻¹ (39%)	0.42 ng g ⁻¹	0.42 ng g ⁻¹ (23%)	1.2 ng g ⁻¹ (48%)
PBAP	0.57 ng g ⁻¹ (63%)	0.57 ng g ⁻¹	0.77 ng g ⁻¹ (43%)	1.1 ng g ⁻¹ (44%)
Coal	–	0.29 ng g ⁻¹	0.28 ng g ⁻¹ (16%)	0.1 ng g ⁻¹ (4%)
Pig Iron	–	0.13 ng g ⁻¹	0.35 ng g ⁻¹ (19%)	0.07 ng g ⁻¹ (3%)

Note. Values under parenthesis refer to the contribution of each source to total P concentrations. The crustal contribution was calculated using Ce data (Section 3.2). The contribution of coal burning and pig iron were calculated from the estimated deposition fluxes reported in Figure 6. The contribution of PBAP (0.57 ng g⁻¹ during PI) was assumed to reach 1.1 ng g⁻¹ from 1975 to 2000 (see text).

Data Availability Statement

Ice core data are available at NCEI (National Centers for Environmental Information) data base (<https://www.ncei.noaa.gov/access/paleo-search/study/38041>).

Acknowledgments

The ice-core drilling operations at CDD were supported by the European Community ENV4-CT97 (ALPCLIM) contract. The LEFE-CHAT (CNRS) program entitled “Evolution séculaire de la charge et composition de l’aérosol organique au-dessus de l’Europe (ESCCARGO)” was supported by ADEME (Agence de l’Environnement et de la Maîtrise de l’Energie). NSF Grant 1925417 to JRM provided partial support for the analyses and interpretation at DRI. We thank colleagues who participated in the drilling campaigns at CDD. We thank the reviewers whose comments improved the manuscript.

References

- Arienzo, M. M., Legrand, M., Preunkert, S., Stohl, A., Chellman, N., Eckhardt, S., et al. (2021). Alpine ice-core evidence of a large increase in vanadium and molybdenum pollution in Western Europe during the 20th century. *Journal of Geophysical Research: Atmospheres*, *126*(4), e2020JD033211. <https://doi.org/10.1029/2020JD033211>
- Arienzo, M. M., McConnell, J. R., Chellman, N., & Kipfstuhl, S. (2019). Method for correcting continuous ice-core elemental measurements for under-recovery. *Environmental Science & Technology*, *53*(10), 5887–5894. <https://doi.org/10.1021/acs.est.9b00199>
- Bergametti, G., Martin, D., Carbonnelle, J., & Vié Le Sage, R. (1984). A mesoscale study of the elemental composition of aerosols emitted from Mt Etna. *Bulletin Volcanologique*, *47*–2(2), 1107–1114. <https://doi.org/10.1007/bf01952366>
- Boulaine, J. (1995). Quatre siècles de fertilization. *Étude et Gestion des Sols*, *2*(4), 219–226.
- Bowen, H. (1966). *Trace elements in biochemistry*. Academic Press.
- Brahney, J., Mahowald, N., Ward, D. S., Ballantyne, A. P., & Neff, J. C. (2015). Is atmospheric phosphorus pollution altering global alpine Lake stoichiometry? *Global Biogeochemical Cycles*, *29*(9), 1369–1383. <https://doi.org/10.1002/2015GB005137>
- British Petroleum. (2020). Energy charting tool—App. Retrieved from <https://www.bp.com/en/global/corporate/energy-economics/energy-charting-tool-desktop.html>
- Broecker, W. S. (1982). Ocean chemistry during glacial time. *Geochimica et Cosmochimica Acta*, *46*(10), 1689–1705. [https://doi.org/10.1016/0016-7037\(82\)90110-7](https://doi.org/10.1016/0016-7037(82)90110-7)
- Calabrese, S., Aiuppa, A., Allard, P., Bagnato, E., Bellomo, S., Brusca, L., et al. (2011). Atmospheric sources and sinks of volcanogenic elements in a basaltic volcano (Etna, Italy). *Geochimica et Cosmochimica Acta*, *75*(23), 7401–7425. <https://doi.org/10.1016/j.gca.2011.09.040>
- Carlson, B. Z., Corona, M. C., Dentant, C., Bonet, R., Thuiller, W., & Choler, P. (2017). Observed long-term greening of alpine vegetation—A case study in the French Alps. *Environmental Research Letters*, *12*(11), 114006. <https://doi.org/10.1088/1748-9326/aa84bd>
- Cinotti, B. (1996). Évolution des surfaces boisées en France: Proposition de reconstitution depuis le début du XIXe siècle. *Revue Forestière Française*, *48*(6), 547–562. <https://doi.org/10.4267/2042/26776>
- De Angelis, M., & Gaudichet, A. (1991). Saharan dust deposition over Mont Blanc (French Alps) during the last 30 years. *Tellus Series B Chemical and Physical Meteorology*, *43*(1), 61–75. <https://doi.org/10.3402/tellusb.v43i1.15246>
- Desboeufs, K., Bon Nguyen, E., Chevaillier, S., Triquet, S., & Dulac, F. (2018). Fluxes and sources of nutrient and trace metal atmospheric deposition in the northwestern Mediterranean. *Atmospheric Chemistry and Physics*, *18*(19), 14477–14492. <https://doi.org/10.5194/acp-18-14477-2018>
- Després, V. R., Huffman, J. A., Burrows, S. M., Hoose, C., Safatov, A. S., Buryak, G., et al. (2012). Primary biological aerosol particles in the atmosphere: A review. *Tellus B: Chemical and Physical Meteorology*, *64*(1), 15598. <https://doi.org/10.3402/tellusb.v64i0.15598>
- Eckhardt, S., Cassiani, M., Evangeliou, N., Sollum, E., Pisso, I., & Stohl, A. (2017). Source-receptor matrix calculation for deposited mass with the Lagrangian particle dispersion model FLEXPART v10.2 in backward mode. *Geoscientific Model Development*, *10*(12), 4605–4618. <https://doi.org/10.5194/gmd-10-4605-2017>
- Environmental Protection Agency. (1973). National emissions inventory of sources and emissions of phosphorus. EPA-450/3-74-013.
- Fagerli, H., Legrand, M., Preunkert, S., Vestreng, V., Simpson, D., & Cerqueira, M. (2007). Modeling historical long-term trends of sulfate, ammonium, and elemental carbon over Europe: A comparison with ice core records in the Alps. *Journal of Geophysical Research*, *112*(D23), D23S13. <https://doi.org/10.1029/2006JD008044>
- Garivait, S., Quisefit, J.-P., de Chateaubourg, P., & Malingre, G. (1997). Multi-element analysis of plants by WDXRF using the scattered radiation correction method. *X-Ray Spectrometry*, *26*(5), 257–264. [https://doi.org/10.1002/\(sici\)1097-4539\(199709\)26:5<257::aid-xrs199>3.0.co;2-6](https://doi.org/10.1002/(sici)1097-4539(199709)26:5<257::aid-xrs199>3.0.co;2-6)
- Garivait, S., Quisefit, J. P., Steiner, E., & de Châteaubourg, P. (1996). La spectrométrie de fluorescence X pour l’analyse quantitative des végétaux et de leurs produits résiduels de combustion. *Journal de Physique*, *6*(C4), 823–832. <https://doi.org/10.1051/jp4:1996479>
- Graham, W. F., & Duce, R. A. (1979). Atmospheric pathways of the phosphorus cycle. *Geochimica et Cosmochimica Acta*, *43*(8), 1195–1208. [https://doi.org/10.1016/0016-7037\(79\)90112-1](https://doi.org/10.1016/0016-7037(79)90112-1)
- Graham, W. F., Piotrowicz, S. R., & Duce, R. A. (1979). The sea as a source of atmospheric phosphorus. *Marine Chemistry*, *7*(4), 325–342. [https://doi.org/10.1016/0304-4203\(79\)90019-7](https://doi.org/10.1016/0304-4203(79)90019-7)
- Guha, M. M., & Mitchell, R. L. (1966). The trace and major elements composition of the leaves of some deciduous trees. *Plant and Soil*, *24*(1), 90–112. <https://doi.org/10.1007/bf01373076>
- Hersbach, H., Bell, B., Berrisford, P., Hirahara, S., Horanyi, A., Munoz-Sabater, J., et al. (2020). The ERA5 global reanalysis. *Quarterly Journal of the Royal Meteorological Society*, *146*(730), 1999–2049. <https://doi.org/10.1002/qj.3803>
- Hoose, C., Kristjánsson, J. E., & Burrows, S. M. (2010). How important is biological ice nucleation in clouds on a global scale? *Environmental Research Letters*, *5*(2), 024009. <https://doi.org/10.1088/1748-9326/5/2/024009>
- Jaenicke, R. (2005). Abundance of cellular material and proteins in the atmosphere. *Science*, *308*(5718), 73. <https://doi.org/10.1126/science.1106335>
- Kanakidou, M., Duce, R. A., Prospero, J. M., Baker, A. R., Benitez-Nelson, C., Dentener, F. J., et al. (2012). Atmospheric fluxes of organic N and P to the global ocean. *Global Biogeochemical Cycles*, *26*(3), GB3026. <https://doi.org/10.1029/2011GB004277>
- Legrand, M., McConnell, J. R., Bergametti, G., Preunkert, S., Chellman, N., Desboeufs, K., et al. (2023a). Alpine-ice record of bismuth pollution implies a major role of military use during World War II. *Scientific Reports*, *13*(1), 1166. <https://doi.org/10.1038/s41598-023-28319-3>
- Legrand, M., McConnell, J. R., Chellman, N., & Preunkert, S. (2023b). Col du Dome ice core phosphorus data from 1892–2000 CE and preindustrial phosphorus and manganese [Dataset]. NCEI. <https://www.ncei.noaa.gov/access/paleo-search/study/38041>
- Legrand, M., McConnell, J. R., Lestel, L., Preunkert, S., Arienzo, M., Chellman, N. J., et al. (2020). Cadmium pollution from zinc-smelters up to fourfold higher than expected in Western Europe in the 1980s as revealed by alpine ice. *Geophysical Research Letters*, *47*(10), e2020GL087537. <https://doi.org/10.1029/2020GL087537>
- Legrand, M., McConnell, J. R., Preunkert, S., Arienzo, M., Chellman, N., Gleason, K., et al. (2018). Alpine ice evidence of a three-fold increase in atmospheric iodine deposition since 1950 in Europe due to increasing oceanic emissions. *Proceedings of the National Academy of Sciences of the United States of America*, *115*(48), 12136–12141. <https://doi.org/10.1073/pnas.1809867115>

- Legrand, M., McConnell, J. R., Preunkert, S., Bergametti, G., Chellman, N. J., Desboeufs, K., et al. (2022). Thallium pollution in Europe over the twentieth century recorded in Alpine ice: Contributions from coal burning and cement production. *Geophysical Research Letters*, 49(13), e2022GL098688. <https://doi.org/10.1029/2022GL098688>
- Legrand, M., Preunkert, S., Wagenbach, D., & Fischer, H. (2002). Seasonally resolved Alpine and Greenland ice core records of anthropogenic HCl emissions over the 20th century. *Journal of Geophysical Research*, 107(D12), 4139. <https://doi.org/10.1029/2001JD001165>
- Loÿe-Pilot, M.-D., & Martin, J.-M. (1996). Saharan dust input to the western Mediterranean: An eleven years record in Corsica. In S. Guerzoni & R. Chester (Eds.), *The impact of desert dust across the Mediterranean* (pp. 191–199). Kluwer. https://doi.org/10.1007/978-94-017-3354-0_18
- Mahowald, N., Jickells, T. D., Baker, A. R., Artaxo, P., Benitez-Nelson, C. R., Bergametti, G., et al. (2008). Global distribution of atmospheric phosphorus sources, concentrations and deposition rates, and anthropogenic impacts. *Global Biogeochemical Cycles*, 22(4), GB4026. <https://doi.org/10.1029/2008GB003240>
- Masson, D., & Frei, C. (2016). Long-term variations and trends of mesoscale precipitation in the Alps: Recalculation and update for 1901–2008. *International Journal of Climatology*, 36(1), 492–500. <https://doi.org/10.1002/joc.4343>
- McConnell, J. R., Chellman, N. J., Wilson, A. I., Stohl, A., Arienzo, M. M., Eckhardt, S., et al. (2019). Pervasive Arctic lead pollution suggests substantial growth in medieval silver production modulated by plague, climate, and conflict. *Proceedings of the National Academy of Sciences of the United States of America*, 116(30), 14910–14915. <https://doi.org/10.1073/pnas.1904515116>
- Mitchell, B. (1975). *European historical statistics* (pp. 1750–1970). Palgrave Macmillan UK. <https://doi.org/10.1007/978-1-349-01088-2>
- Myriokefalitakis, S., Nenes, A., Baker, A. R., Mihalopoulos, N., & Kanakidou, M. (2016). Bioavailable atmospheric phosphorus supply to the global ocean: A 3-D global modeling study. *Biogeosciences*, 13(24), 6519–6543. <https://doi.org/10.5194/bg-13-6519-2016>
- Nriagu, J. O. (1989). A global assessment of natural sources of atmospheric trace metals. *Nature*, 338(6210), 47–49. <https://doi.org/10.1038/338047a0>
- Pacyna, J. (1991). *Emission factors of atmospheric Cd, Pb and Zn for major source categories in Europe during 1950–1985* Technical Report NILU-OR-30/91 (p. 34). Norwegian Institute for Air Research.
- Pacyna, J. M., & Pacyna, E. G. (1999). Atmospheric emissions of anthropogenic lead in Europe: Improvements, updates, historical data and projections. Technical Report 2000/31 for GKSS Research Center.
- Pacyna, J. M., Pacyna, E. G., & Aas, W. (2009). Changes of emissions and atmospheric deposition of mercury, lead, and cadmium. *Atmospheric Environment*, 43(1), 117–127. <https://doi.org/10.1016/j.atmosenv.2008.09.066>
- Pilson, M. E. Q. (1998). *An introduction to the chemistry of the sea* (2nd ed.). Cambridge University Press.
- Pisso, I., Sollum, E., Grythe, H., Kristiansen, N. I., Cassiani, M., Eckhardt, S., et al. (2019). The Lagrangian particle dispersion model FLEX-PART version 10.4. *Geoscientific Model Development*, 12, 4955–4997. <https://doi.org/10.5194/gmd-12-4955-2019>
- Preunkert, S., & Legrand, M. (2013). Towards a quasi-complete reconstruction of past atmospheric aerosol load and composition (organic and inorganic) over Europe since 1920 inferred from alpine ice cores. *Climate of the Past*, 9(4), 1403–1416. <https://doi.org/10.5194/cp-9-1403-2013>
- Preunkert, S., McConnell, J. R., Hoffmann, H., Legrand, M., Wilson, A. I., Eckhardt, S., et al. (2019). Lead and antimony in basal ice from Col du Dome (French Alps) dated with radiocarbon: A record of pollution during antiquity. *Geophysical Research Letters*, 46(9), 4953–4961. <https://doi.org/10.1029/2019GL082641>
- Preunkert, S., Wagenbach, D., Legrand, M., & Vincent, C. (2000). Col du Dome (Mt Blanc Massif, French Alps) suitability for ice-core studies in relation with past atmospheric chemistry over Europe. *Tellus Series B Chemical and Physical Meteorology*, 52(3), 993–1012. <https://doi.org/10.3402/tellusb.v52i3.17081>
- Puxbaum, H., & Tenze-Kunit, M. (2003). Size distribution and seasonal variation of atmospheric cellulose. *Atmospheric Environment*, 37(26), 3693–3699. [https://doi.org/10.1016/s1352-2310\(03\)00451-5](https://doi.org/10.1016/s1352-2310(03)00451-5)
- Sánchez-Ochoa, A., Kasper-Giebl, A., Puxbaum, H., Gelencser, A., Legrand, M., & Pio, C. (2007). Concentration of atmospheric cellulose: A proxy for plant debris across a west-east transect over Europe. *Journal of Geophysical Research*, 112(D23), D23S08. <https://doi.org/10.1029/2006JD008180>
- Swaine, D. J. (1990). *Trace elements in coal*. Butterworths.
- Taha, E.-L. A., & Al-Kahtani, S. (2020). Macro- and trace elements content in honeybee pollen loads in relation to the harvest season. *Saudi Journal of Biological Sciences*, 27(7), 1797–1800. <https://doi.org/10.1016/j.sjbs.2020.05.019>
- U.S. Geological Survey Statistics. (n.d.). National Minerals Information Center. Retrieved from <https://www.usgs.gov/centers/national-minerals-information-center/minerals-yearbook-metals-and-minerals>
- Wang, R., Balkanski, Y., Boucher, O., Ciaia, P., Peñuelas, J., & Tao, S. (2015). Significant contribution of combustion-related emissions to the atmospheric phosphorus budget. *Nature Geoscience*, 8(1), 48–54. <https://doi.org/10.1038/ngeo2324>
- Xu, J., Shen, G., Fu, B., Han, Y., Suo, X., Chen, Z., et al. (2023). Emissions of particulate and previously ignored gaseous phosphorus from coal and biomass combustion in household stoves. *Environmental Science and Technology Letters*. <https://doi.org/10.1021/acs.estlett.3c00029>

References From the Supporting Information

- British Geological Survey. (2020). World mineral statistics. <https://www2.bgs.ac.uk/mineralsuk/statistics/wms.cfc?method=searchWMS>
- Wagenbach, D., Preunkert, S., Schäfer, J., Jung, W., & Tomadin, L. (1996). Northward transport of Saharan dust recorded in a deep alpine ice core. In S. Guerzoni & R. Chester (Eds.), *The impact of desert dust across the Mediterranean* (pp. 291–300). Kluwer Academic Publishers. https://doi.org/10.1007/978-94-017-3354-0_29